

# Spontaneous fission and alpha-decay properties of neutron deficient isotopes $^{257-253}104$ and $^{258}106$

F.P.Heßberger<sup>1</sup>, S.Hofmann<sup>1</sup>, V.Ninov<sup>1</sup>, P.Armbruster<sup>1</sup>, H.Folger<sup>1</sup>, G.Münzenberg<sup>1</sup>, H.J.Schött<sup>1</sup>, A.G.Popeko<sup>2</sup>, A.V.Yeremin<sup>2</sup>, A.N.Andreyev<sup>2</sup>, S.Saro<sup>3</sup>

<sup>1</sup> Gesellschaft für Schwerionenforschung mbH, D-64220 Darmstadt, Germany

<sup>2</sup> Flerov Laboratory of Nuclear Reactions, JINR, 141890 Dubna, Russia

<sup>3</sup> Department of Nuclear Physics, Comenius University, SK-84215 Bratislava, Slovakia

Received: 20 June 1997 / Revised version: 13 August 1997

Communicated by V. Metag

**Abstract.** Spontaneous fission and  $\alpha$ -decay of  $^{253-257}104$  and  $^{258}106$  were investigated in irradiations of  $^{204,206,208}\text{Pb}$  with  $^{50}\text{Ti}$  and  $^{209}\text{Bi}$  with  $^{51}\text{V}$ , respectively. New spontaneous fission activities were identified and assigned to  $^{253}104$ ,  $^{254}104$ , and  $^{258}106$ . The half-lives were measured as  $T_{1/2} = (48_{-10}^{+17}) \mu\text{s}$  for  $^{253}104$ ,  $T_{1/2} = (23 \pm 3) \mu\text{s}$  for  $^{254}104$ , and  $T_{1/2} = (2.9_{-0.7}^{+1.3}) \text{ms}$  for  $^{258}106$ . No indication for  $\alpha$ -decay of any of these isotopes was found. For the  $\alpha$ -decay branching ratios  $b_\alpha$  limits corresponding to  $b_\alpha \leq 0.1$  for  $^{253}104$ ,  $b_\alpha \leq 0.015$  for  $^{254}104$ , and  $b_\alpha \leq 0.2$  for  $^{258}106$  were obtained. These results prove a reduced fission probability for nuclei with neutron numbers  $N=152$  up to  $Z=106$  and a steep decrease of the fission half-lives for neutron numbers  $N < 152$  up to element 104.

$\alpha$ -decay data of  $^{257}104$  and  $^{255}104$  have been improved. An isomeric state decaying by  $\alpha$ -emission was identified in  $^{257}104$  and attributed to a low lying  $11/2^- [725]$  state. A small  $\alpha$ -decay branch for the even - even nucleus  $^{256}104$ , indicated in an earlier experiment at SHIP, was confirmed, allowing a better founded extrapolation of experimental masses for even - even nuclei up to  $^{264}\text{Hs}$  ( $Z=108$ ), the heaviest even - even nucleus identified so far.

**PACS:** 27.90.+b; 23.60.+e; 25.85.Ca; 25.70.Jj

## 1 Introduction

In the region of the heaviest elements, where the liquid drop fission barrier tends to decrease to zero, nuclear shell structure is of special importance for the stability of nuclei. Experimentally, the influence of the neutron subshell at  $N=152$  on the fission half-lives was recognized already long ago (see e.g. [1]). The enhanced stability against spontaneous fission at  $N=152$  is especially striking for fermium ( $Z=100$ ) and nobelium ( $Z=102$ ) isotopes (Fig. 1). Therefore, the steep decrease in spontaneous fission half-lives by roughly seven orders of magnitude from  $^{254}\text{No}$  ( $T_{sf} = 2.2 \times 10^4 \text{ s}$  according to a recent measurement [2]) to  $^{256}104$  ( $T_{sf} \approx 5 \text{ ms}$  [3]) was unexpected and led to controversy concerning the interpretation of the data [4]. However, assignment and half-life of  $^{256}104$  were later confirmed [5]. The drastic change in the half-lives

from  $Z=102$  to  $Z=104$  was explained in [3] by the decrease of the outer fission barrier below the groundstate. This effect was quantitatively connected to a significant increase of the barrier curvature energy  $\hbar\omega$  [6]. Under these circumstances the steep decrease of the spontaneous fission half-lives from  $^{254}\text{No}$  to  $^{256}104$  cannot be regarded as a signature for the disappearance of the deformed neutron shell at  $N=152$  for  $Z > 102$ . Indeed,  $Q_\alpha$  -values for isotopes of  $Z=104$  to  $Z=106$  around  $N=152$  do not give a hint of such an effect [5, 7, 8]. Instead, rather constant fission half-lives are evident at  $Z=104$  for neutron numbers  $N=152-156$ , and also for  $^{260}106$  with  $N=154$ . Thus an extension of experimental fission half-lives to lower neutron numbers seems desirable. Therefore one aim of our experiment was to check the results from [9] concerning the isotope  $^{254}104$  as well as to search for the decay properties of the new isotope  $^{258}106$ .

While for the even-even isotopes of element 104 spontaneous fission practically is the exclusive decay mode, the odd mass nuclei predominantly decay by  $\alpha$ - emission. Detailed

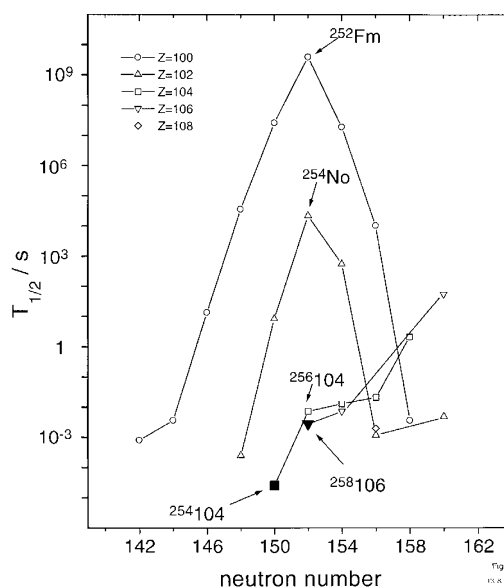


**Fig. 1.** Systematics of fission half-lives for even - even nuclei. The new data are marked by filled symbols. Literature values are taken from [2]( $^{254}\text{No}$ ), [36]( $^{262}104$ ), [37]( $^{266}106$ ), [31]( $^{264}\text{Hs}$ ) or [32]

$\alpha$ -spectroscopic investigations of  $Z=104$  - isotopes have not been reported up to now, partly because the experiments were not sensitive to  $\alpha$ -decay, partly because the background of nuclei with  $Z < 104$ , produced by transfer reaction was disturbingly high, and partly because the count rates were too small. As a first step to overcome this shortage we chose the isotope  $^{257}104$ , which is interesting for such studies since it a) continues the line of the  $N=153$  nuclei  $^{251}\text{Cf}$ ,  $^{253}\text{Fm}$ , for which detailed  $\alpha$ -decay studies are available, b) is reported to have a complicated  $\alpha$ -decay pattern, and c) has a production cross section of several nanobarns for the reaction  $^{208}\text{Pb}(^{50}\text{Ti},n)^{257}104$ , allowing to produce a large number ( $>1000$ ) of nuclei within reasonable irradiation times.

## 2 Experimental set-up

The experiments were performed with beams of  $^{50}\text{Ti}$  or  $^{51}\text{V}$  from the UNILAC accelerator at GSI, Darmstadt. Beam intensities up to  $4 \times 10^{12}$  ( $\approx 650$  particle nA) were used. The targets of  $^{204,206,208}\text{Pb}$  or  $^{209}\text{Bi}$  (thickness:  $450\text{--}500 \mu\text{g}/\text{cm}^2$ , covered with carbon layers of  $40 \mu\text{g}/\text{cm}^2$  (upstream) and  $5 \mu\text{g}/\text{cm}^2$  (downstream)) were mounted on a wheel rotating synchronously to the beam macro structure [10]. The evaporation residues, recoiling from the target with kinetic energies of  $\approx 0.17 \times A$  MeV, were separated from the projectile beam in-flight by the velocity filter SHIP [11]. SHIP was extended by a  $7.5^\circ$  deflection dipole magnet, installed downstream the second quadrupole triplet. This arrangement improved the suppression of background, e.g. scattered  $^{50}\text{Ti}$ ,  $^{51}\text{V}$  projectiles of low energy or target-like transfer products, by a factor of roughly 100. Before the evaporation residues were finally implanted into a position sensitive 16-strip silicon wafer ('stop detector') they passed a time-of-flight system, consisting of two transmission detectors [12]. The stop detector had an active area of  $80 \times 35 \text{ mm}^2$ . It was used to measure the kinetic energy of the incoming particles as well as to register  $\alpha$ -decay or spontaneous fission of implanted nuclei. In front of the stop detector there was a holder for calibration sources and mylar degrader foils to absorb the residual background of scattered low energy projectiles. The energy resolution of the detector was measured to be  $\Delta E = 14 \text{ keV}$  for  $\alpha$ -particles from a  $^{241}\text{Am}$  source; for  $\alpha$ -particles emitted from implanted nuclei it was somewhat worse due to partly registering the recoil energy transferred to the residual nucleus by the  $\alpha$ -particle. A value of  $\Delta E = 18 \text{ keV}$  was measured for  $\alpha$ -particles from  $^{211}\text{Po}$ , produced by few nucleon transfer reactions and registered as 'background'. The time-of-flight system served both to discriminate between incoming particles and decays within the stop detector ('anticoincidence'), and to give a rough mass estimate for the incoming nuclei via a kinetic energy - time-of-flight - measurement. Further details on the experimental set-up are given in [13].

## 3 Experimental results and discussion

### 3.1 Irradiations of $^{204,206,208}\text{Pb}$ with $^{50}\text{Ti}$

#### 3.1.1 Excitation functions

The production of evaporation residues (ER) was measured with the excitation energy  $E^*$  of the compound nuclei ranging

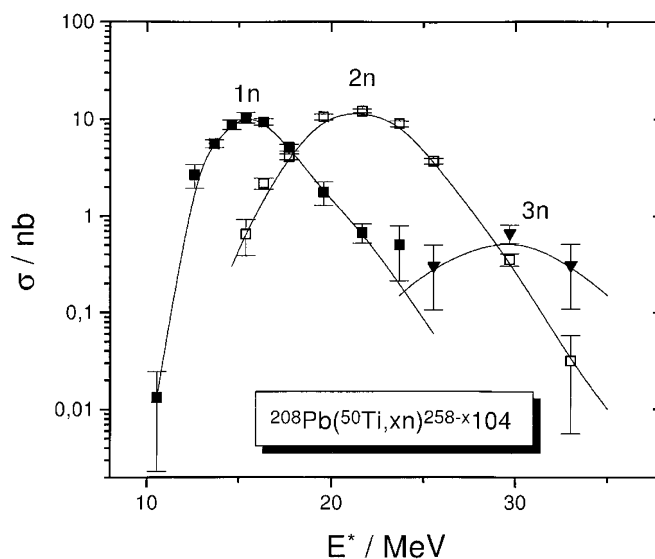


Fig. 2. Excitation functions for evaporation residue production in irradiations of  $^{208}\text{Pb}$  with  $^{50}\text{Ti}$ . The lines are to guide the eye

from  $E^* = 10.6 \text{ MeV}$  to  $E^* = 33.0 \text{ MeV}$ . The  $E^*$  values of the compound nuclei, calculated by using mass excess data from [14], refer to a production in the center of the target. The energy loss of the projectiles in the upstream carbon layer and the first half of the target was  $\Delta E \approx 2.8 \text{ MeV}$  according to [15]. Products from 1n-, 2n- and 3n- deexcitation could be observed. The decay properties of the corresponding isotopes  $^{257}104$  [16, 17, 5],  $^{256}104$  [3, 5], and  $^{255}104$  [3, 5] are known from the literature. Nevertheless improved decay data could be obtained. The maxima of the production cross section  $\sigma_{max}$ , observed at  $E^* = (15.6 \pm 0.1) \text{ MeV}$  (1n),  $E^* = (21.5 \pm 0.1) \text{ MeV}$  (2n), and  $E^* = (29 \pm 1) \text{ MeV}$  (3n), were  $\sigma_{max,1n} = (10 \pm 1) \text{ nb}$ ,  $\sigma_{max,2n} = (12 \pm 1) \text{ nb}$ , and  $\sigma_{max,3n} = (0.7 \pm 0.5) \text{ nb}$ . The uncertainties stem from statistical contributions only. Systematic uncertainties introduced by the calculated efficiency (40%) of the set-up are not included. They may be estimated as being of the order of 50%. The complete excitation functions are shown in Fig. 2. They appear to be narrow. Widths of  $(4.3 \pm 0.2) \text{ MeV}$  (FWHM) for the 1n-deexcitation channel and  $(6.3 \pm 0.6) \text{ MeV}$  (FWHM) for the 2n-deexcitation channel have been obtained from fits to the measured cross sections.

#### 3.1.2 Isotope $^{257}104$

The first identification of  $^{257}104$  was reported by Ghiorso et al. [16]. Four  $\alpha$ -lines in the region  $E = (8.7\text{--}8.9) \text{ MeV}$ , which they observed in the bombardment of  $^{249}\text{Cf}$  with  $^{12}\text{C}$ , were assigned to this isotope. A half-life of  $T_{1/2} = (4.5 \pm 1.0) \text{ s}$  was measured. Later, Bemis et al. [17] used the same reaction to produce this  $\alpha$ -emitter and to assign it unambiguously to element 104 by  $\alpha$ -X-ray-coincidence measurements. A total of nine  $\alpha$ -lines was attributed to this isotope.

In our first attempt [5] to synthesize element 104 in bombardments of  $^{208}\text{Pb}$  with  $^{50}\text{Ti}$ , a total of 18  $\alpha$ -decays, attributed to  $^{257}104$ , was observed, five of them being correlated to  $^{253}\text{No}$ . The complex structure of its  $\alpha$ -spectrum was confirmed, although, due to the low number of observed events,

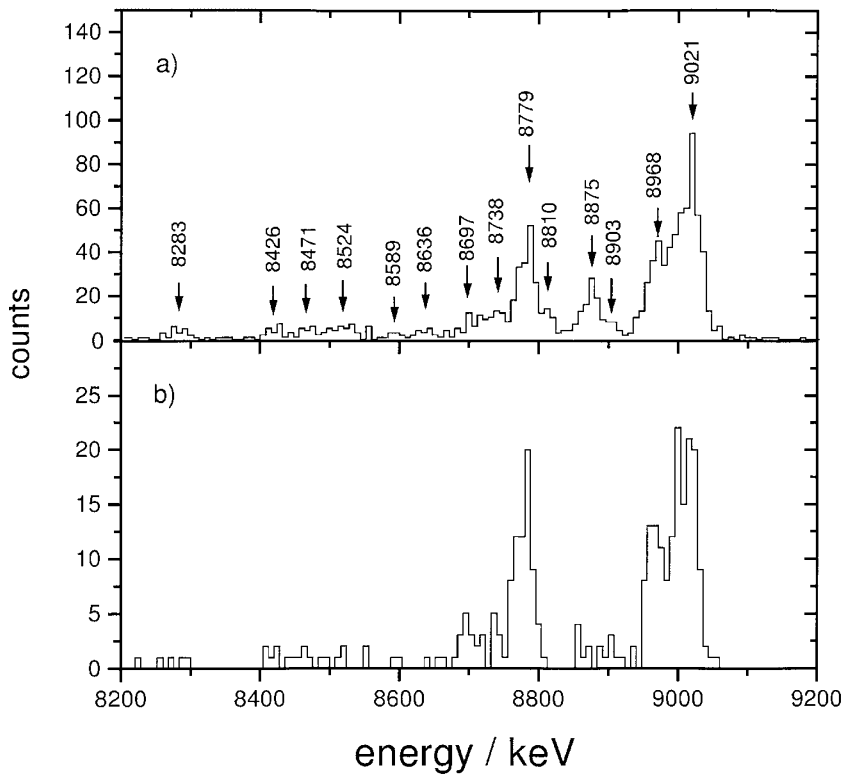


**Fig. 3.** Spectrum of  $\alpha$ -particles attributed to  $^{257}104$  from  $^{50}\text{Ti} + ^{208}\text{Pb}$  at  $E_{proj} = (4.52-4.81) \times A$  MeV **a** correlated to evaporation residues **b** correlated to daughter decays ( $E_{\alpha} = 7950 - 8200$  keV)

two of the attributed lines consisted only of one event each [5].

In the present experiment we observed a total of about 1100  $\alpha$ -decays in the region  $E_{\alpha} = (8200-9100)$  keV that could be attributed predominantly to  $^{257}104$  or its EC-decay daughter  $^{257}\text{Lr}$  [18, 19]. About 30% of these events were followed by  $\alpha$ -decays in the region  $E_{\alpha} = (7900-8200)$  keV, which were assigned to  $^{253}\text{No}$  [20, 21]. The spectrum of  $\alpha$ -decays is shown in Fig. 3. On the basis of the measured  $\alpha$ -resolution of  $\Delta E(\text{FWHM}) = 18$  keV the measured  $\alpha$ -events could be attributed to 15 lines (Table 1). The  $\alpha$ -lines at 8283, 8426, 8471, 8697, 8738, 8779, 8810, 8968 and 9021 keV were assigned unambiguously to  $^{257}104$  by establishing delayed  $\alpha$ - $\alpha$ -coincidences with the daughter  $^{253}\text{No}$ . On the basis of a detailed analysis of the  $\alpha$ -decays two of these lines ( $E_{\alpha} = 8968, 9021$  keV) were attributed to an isomeric state  $^{257m}104$  (see Sect. 3.3). Therefore we shall restrict the following discussion to the remaining ones.

8524 keV: the line was found to be rather broad with  $\Delta E = 65$  keV ( $3.6 \times \text{FWHM}$ ), so that it probably represents an unresolved doublet.

8589 keV: only one of eight observed events was correlated to  $^{253}\text{No}$ . Thus an assignment to  $^{257}104$  on the basis of our present data is questionable.

8636 keV: none of the 16 events observed is correlated to  $^{253}\text{No}$ . Therefore this line cannot be attributed to  $^{257}104$ .  $\alpha$ -decay energies close to this value are known for  $^{258}\text{Lr}$  [18, 19] and for  $^{256}\text{Lr}$  [19], yet an assignment to any of these nuclei was not likely.  $^{258}\text{Lr}$  cannot be produced directly in that reaction, since its neutron number is by one higher than that of the compound nucleus  $^{258}104$ . A production via  $\gamma$ -deexcitation followed by EC-decay of  $^{258}104$  can be

**Table 1.** List of  $\alpha$ -lines observed in  $^{50}\text{Ti} + ^{208}\text{Pb}$  and assigned to element 104 isotopes or daughter products. <sup>a</sup> = tentative assignment, <sup>b</sup> = including one event from [5], <sup>c</sup> = only correlated events

$E_{\alpha}/\text{keV}$	$\Sigma_{\alpha}$	$i_{rel}$	$T_{1/2}/\text{s}$	assignment
8283	17	$0.04 \pm 0.01$	$2.1^{+0.7}_{-0.4}$	$^{257}104$
8426	18	$0.05 \pm 0.01$	$4.0^{+1.4}_{-0.8}$	$^{257}104$
8471	17	$0.04 \pm 0.01$	$3.0^{+1.1}_{-0.6}$	$^{257}104$
8524	35	$0.09 \pm 0.02$	$3.3^{+0.8}_{-0.5}$	$^{257}104$
8589	8	$0.02 \pm 0.01$	$3.6^{+1.9}_{-0.9}$	$^{257}104^a$
8697	30	$0.08 \pm 0.01$	$3.5^{+1.0}_{-0.6}$	$^{257}104$
8738	58	$0.15 \pm 0.02$	$4.2 \pm 0.7$	$^{257}104$
8779	176	$0.44 \pm 0.03$	$3.5 \pm 0.3$	$^{257}104$
8864	14	$0.03 \pm 0.01$	$2.7^{+2.4}_{-0.8}$	$^{257}104$
8903	23	$0.06 \pm 0.01$	$3.6^{+1.2}_{-0.7}$	$^{257}104$
8968	251	$0.44 \pm 0.03$	$3.6 \pm 0.3$	$^{257m}104$
9021	325	$0.56 \pm 0.03$	$4.4 \pm 0.4$	$^{257m}104$
8636	16	$0.14 \pm 0.04$	$4.8^{+2.0}_{-1.1}$	$^{257}\text{Lr}^a$
8810	23	$0.20 \pm 0.04$	$4.3^{+1.3}_{-0.8}$	$^{257}\text{Lr}$
8875	74	$0.66 \pm 0.08$	$3.3^{+0.5}_{-0.4}$	$^{257}\text{Lr}$
8011	90	$0.33 \pm 0.03$	$80 \pm 9$	$^{253}\text{No}$
8038	83	$0.31 \pm 0.03$	$74 \pm 9$	$^{253}\text{No}$
8063	74	$0.28 \pm 0.03$	$72 \pm 8$	$^{253}\text{No}$
8114	20	$0.08 \pm 0.02$	$83^{+24}_{-15}$	$^{253}\text{No}$
8790	4 <sup>b</sup>		$(5.0^{+4.5}_{-1.6}) \times 10^{-3}$	$^{256}104$
8713	5		$1.4^{+1.0}_{-0.4}$	$^{255}104$
8739	8		$2.4^{+1.3}_{-1.1}$	$^{255}104$
8768	9		$1.3^{+0.7}_{-0.4}$	$^{255}104$
8805	4		$1.8^{+1.6}_{-0.6}$	$^{255}104$
8905	3		$1.4^{+6.6}_{-0.6}$	$^{255}104$
8623	15 <sup>c</sup>		$1.0 \pm 0.3$	$^{251}\text{No}$
8725	13		$0.8 \pm 0.3$	$^{255m}104^a$
8482	2 <sup>c</sup>		$0.9^{+1.6}_{-0.3}$	$^{251m}\text{No}^a$

**Table 2.** Comparison of  $\alpha$ -energies attributed to  $^{257}\text{104}$ . The relative intensities are given in brackets

$E_\alpha/\text{keV}$ this work	$E_\alpha/\text{keV}$ [5]	$E_\alpha/\text{keV}$ [17]	$E_\alpha/\text{keV}$ [16]
9021 (0.34)	9012 (0.18)	9016	9000 (0.35)
8968 (0.26)	8977 (0.29)	8951	8950 (0.30)
	8942 (0.12)		
8903 (0.024)	8897 (0.06)		
8864 (0.015)		8870 ( $^{257}\text{Lr}$ )	
8779 (0.18)	8778 (0.06)	8778	8780 (0.20)
8738 (0.060)	8714 (0.18)	8720	8700 (0.15)
8697 (0.031)			
8636 ( $^{257}\text{Lr}$ ?)		8663	
8589 ( $^{257}\text{104}$ ?)	8597 (0.12)	8615	
8524 (0.036)		8553	
8471 (0.018)			
8426 (0.019)			
8283 (0.018)			

excluded, since  $^{258}\text{104}$  is known to decay by spontaneous fission with  $T_{1/2} \approx 11$  ms. No EC-branch is reported for this isotope.  $^{256}\text{Lr}$  could be produced by pn-deexcitation. In this case it should occur together with the 2n-channel. The decays, however, were produced together with the 1n channel at energies below the maximum of the 2n-channel. Thus we tentatively assign this line to  $^{257}\text{Lr}$ , produced by EC-decay of  $^{257}\text{104}$ .

8810 keV: None of the 23  $\alpha$ -decays is correlated to  $^{253}\text{No}$ . The energy agrees with the value reported for the low energy line of  $^{257}\text{Lr}$  [19].

8870 keV: About 10% of the events contributing to this energy, which was previously assigned to  $^{257}\text{Lr}$  [18, 19], are correlated to  $^{253}\text{No}$ . We thus interpret this line as a mixture of  $^{257}\text{Lr}$  and  $^{257}\text{104}$ . A comparison between the events correlated to  $^{253}\text{No}$  and the uncorrelated ones results in different mean energies of  $E_\alpha = 8864 \pm 8$  keV for the correlated ones and  $E_\alpha = 8875 \pm 8$  keV for the uncorrelated ones.

Our  $\alpha$ -lines attributed to  $^{257}\text{104}$  are compared with literature values in Table 2. Although in general a fair agreement is obvious, the new data indicate a trend towards about 10–20 keV higher energy values. The relative intensities agree quite well with those obtained by Ghiorso et al. [16], but less well with recent SHIP data [5], which is understandable considering the small number of events observed at that time. The line at  $E_\alpha = 8663$  keV reported by Bemis et al. [17] is probably identical with our line at  $E_\alpha = 8636$  keV, which is not attributed to  $^{257}\text{104}$ , but tentatively to  $^{257}\text{Lr}$ , while the line at  $E_\alpha = 8615$  keV [17], probably identical to our line at  $E_\alpha = 8589$  keV, could not be assigned to  $^{257}\text{104}$  unambiguously. The lines at lower energies ( $E_\alpha < 8500$  keV) have not been reported previously. In our recent experiment [5] they were not observed clearly due to their low intensity, while in the  $^{249}\text{Cf}$ -based reactions [16, 17] the energy region  $E_\alpha = (8200\text{--}8500)$  keV was contaminated by  $\alpha$ -decays of  $^{255}\text{No}$  and  $^{256}\text{No}$ .

The branching ratio for EC decay ( $b_{EC}$ ) of  $^{257}\text{104}$  can be estimated from the total number of  $\alpha$ -decays attributed to this isotope, taking into account that both the groundstate as well as the isomeric state may decay by EC, and those assigned to  $^{257}\text{Lr}$ . A direct production of  $^{257}\text{Lr}$  via p-deexcitation can

be excluded due to the measured 'effective' half-life, which is similar to that of  $^{257}\text{104}$ , an indication for production via EC, whereas in the case of a direct production it would appear with its own half-life of  $T_{1/2} = (0.6 \pm 0.1)$  s [18]. The resulting EC-branch of  $^{257}\text{104}$  is  $b_{EC} = 0.11 \pm 0.01$ .

A fission branch ( $b_{EC}$ ) of  $^{257}\text{104}$  is not unambiguously established. A rather high value of  $b_{sf} = 0.14 \pm 0.09$  is reported by Somerville et al. [22], while our recent experiment did not give a clear indication for spontaneous fission, yielding only a limit  $b_{sf} \leq 0.035$  [5, 23]. The search for spontaneous fission of  $^{257}\text{104}$  in the present experiment was rendered more difficult by background from spontaneous fission of the neighbouring isotope  $^{256}\text{104}$ , the product from the 2n-deexcitation channel. Since thick degrader foils in front of the detector were used to absorb the scattered low energetic projectiles, the energy of the evaporation residues was degraded to apparent mean values close to 5 MeV, i.e. measured values including a reduction of the signals due to the pulse-height defect. Due to a broad energy straggling part of the evaporation residues obviously were registered with energies lower than 2 MeV, i.e. in an energy region that was excluded from the search for ER-sf or ER- $\alpha$  correlations, since it includes the bulk of the low energy, scattered projectiles, which are not fully absorbed in the foils. Thus about 10% of the fission events of  $^{256}\text{104}$  were not correlated to an evaporation residue within 10 s, while about 2.5% of the events were correlated with time distances larger than ten half-lives of  $^{256}\text{104}$ . The latter correlations have to be regarded as random. To estimate an upper  $b_{sf}$  limit of  $^{257}\text{104}$  we used the number of fission events with correlation times  $\Delta t > 50$  ms, corrected for random correlations of  $^{256}\text{104}$ . This procedure is not unambiguous, however, since it assumes that the fraction of random correlations is the same in the maximum of the 2n-channel and the maximum of the 1n-channel; the latter occurs at lower bombarding energies and at lower velocities of the evaporation residues. Thus we regard our value  $b_{sf} \leq 0.014$  as an upper limit.

### 3.1.3 Isotope $^{256}\text{104}$

One  $\alpha$ -decay with an energy of  $E_\alpha = 8812 \pm 23$  keV was attributed to  $^{256}\text{104}$  in our recent paper [5], representing  $b_\alpha = 0.022^{+0.073}_{-0.018}$ . In the present irradiations we observed three more  $\alpha$ -decays having slightly lower individual energies of 8776 keV to 8800 keV. The assignment to  $^{256}\text{104}$  was based either on the measured time difference of  $\Delta t(\text{ER}-\alpha) = 1.1$  ms (one event) or on delayed  $\alpha$ - $\alpha$  coincidences to the daughter products  $^{252}\text{No}$  or  $^{248}\text{Fm}$ . The mean energy value of all four events observed so far is  $E_\alpha = 8790 \pm 20$  keV (see Table 1). In this experiment the total number of fission events of this isotope was approximately 1900 so the improved value is  $b_\alpha = 0.0032 \pm 0.0017$ . From the time distances between implantation of the evaporation residues and the fission events, we determined  $T_{1/2} = 6.2 \pm 0.2$  ms (Fig. 4). This value is slightly lower than, but still in agreement with the previous result of  $T_{1/2} = 7.4^{+0.9}_{-0.7}$  ms [5].

### 3.1.4 Isotope $^{255}\text{104}$

In the current series of experiments the isotope  $^{255}\text{104}$  was produced by the reaction  $^{208}\text{Pb}(^{50}\text{Ti},3n)^{255}\text{104}$  at  $E^* = 33.1, 29.9$

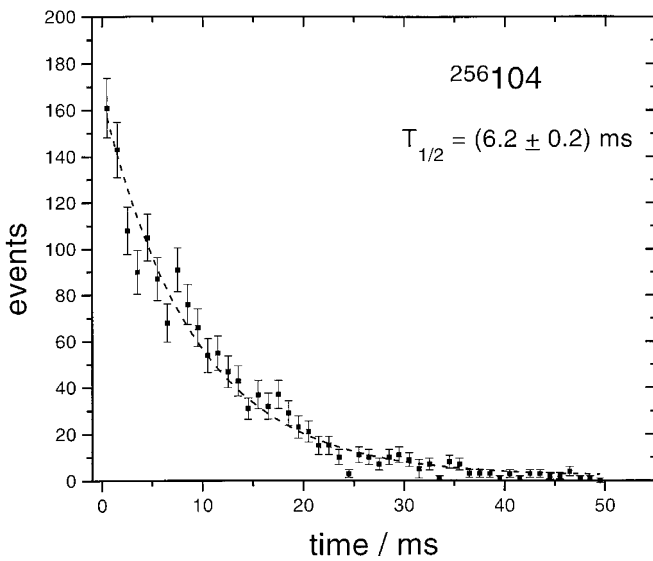


Fig. 4. Time distribution for fission events attributed to  $^{256}104$ . The fitted curve represents an exponential decay curve plus constant background

and 25.7 MeV, and also by the reaction  $^{206}\text{Pb}(^{50}\text{Ti},1n)^{255}104$  at  $E^* = 21.5$  MeV. It was identified by delayed  $\alpha - \alpha$  - coincidences to the known daughter isotope  $^{251}\text{No}$  [21]. The spectrum of  $\alpha$  - particles observed in these reactions and correlated either to evaporation residues within 10 s or to preceding  $\alpha$ -decays within 100 s is displayed in Fig. 5. While the events above 8.7 MeV could predominantly be assigned to  $^{255}104$ , those at 8.6-8.7 MeV are attributed mainly to  $^{251}\text{No}$  and those at 7.8-8.2 MeV to the granddaughter  $^{247}\text{Fm}$  [24]; the broad distribution of the latter events is probably caused by energy summing between  $\alpha$  - particles and conversion electrons [25].

The  $\alpha$  -line at  $E_\alpha = 8623$  keV of  $^{251}\text{No}$  appeared narrow having a width of  $\Delta E$  (FWHM) =  $(15.3 \pm 0.5)$  keV, which even is somewhat smaller than the value of  $\Delta E$  (FWHM) = 18 keV measured for  $^{211}\text{Po}$  (see Sect. 2). It will serve as a reference in the following discussion. According to this value the  $\alpha$ -decays above 8.7 MeV can be divided into four groups: E1 = (8710-8747) keV, E2 = (8750-8795) keV, E3 = (8795-8830) keV and E4 = (8890-8930) keV.

While the decays in the groups E2, E3 and E4 could be assigned unambiguously to  $^{255}104$  by  $\alpha - \alpha$  - correlations, a peculiarity occurred for E1. In Table 3 we have listed the numbers of events and the correlations observed. It is obvious that, although 62% of the  $\alpha$ -decays above 8.7 MeV occur in E1, only 38% of the events correlated to  $^{251}\text{No}$  in the interval (8600-8650) keV are registered in E1. A closer inspection reveals that at best one of the 13 events in the interval (8720-8730) keV is followed by a decay of  $^{251}\text{No}$ ; the energy of this event is 8684 keV, which agrees with a second line of  $^{251}\text{No}$  at  $E_\alpha = 8.68$  MeV [21]. It should be noted, however, that this event is the only one correlated to an event attributed to  $^{255}104$  ( $E_\alpha > 8.7$  MeV) fitting to the second line, although in [21] the intensity of this line is reported as 20%.

$\alpha$  - events correlated to the  $E_\alpha = 8623$  keV line of  $^{251}\text{No}$  are found in E1 only at  $E_\alpha < 8720$  keV or  $E_\alpha > 8730$  keV. It thus seems justified to divide up the  $\alpha$  - events observed in E1 to three groups: Two of them, having mean energies of  $E_\alpha =$

Table 3. list of  $\alpha$ -decays observed at  $^{50}\text{Ti} + ^{208}\text{Pb}$  at  $E = (4.90-5.10) \times A$  MeV and  $^{50}\text{Ti} + ^{206}\text{Pb}$  at  $E = 4.81 \times A$  MeV.  $\Sigma_\alpha$ : events correlated to evaporation residue only;  $\Sigma_{corr}$ : events additionally correlated to  $\alpha$ -decay of  $^{251}\text{No}$  or  $^{247}\text{Fm}$

energy interval (keV)	energy subinterval (keV)	$\Sigma_\alpha$	$\Sigma_{corr}$
8710-8747		26	6
	8710-8720	5	2
	8721-8730	13	1
8750-8795	8731-8747	8	3
		9	6
		4	1
8795-8830		3	3

8713 keV and  $E_\alpha = 8739$  keV, respectively, are attributed to the ground state decay of  $^{255}104$ , as also the events in E2, E3 and E4. The third group, having a mean energy of  $E_\alpha = 8725$  keV evidently does not belong to the same decay pattern. Finally, we want to point out that we observed two correlation chains  $8720 \text{ keV} \rightarrow 8493 \text{ keV}$  and  $8722 \text{ keV} \rightarrow 8471 \text{ keV} \rightarrow 8126 \text{ keV}$ . A meaningful candidate for the corresponding daughter isotope with an  $\alpha$ -decay energy in the region (8450-8500) keV is, however, not known in the literature. The supposition, that the line at  $E_\alpha = 8725$  keV has an origin different from that of the other lines is supported by the time distribution of the events. The half-life of this line is  $T_{1/2} = 0.8_{-0.2}^{+0.5}$  s, while for the other lines a common value of  $T_{1/2} = 1.4_{-0.3}^{+0.5}$  s was obtained.

On the other hand we have to take into account that the  $E_\alpha = 8725$  keV - activity is produced together with the events attributed to  $^{255}104$ . The measured excitation function for  $^{50}\text{Ti} + ^{208}\text{Pb}$  does not indicate a shift of the maximum of its production rate to higher or lower energies, so this activity still has to be connected to the  $3n$  - deexcitation channel of  $^{50}\text{Ti} + ^{208}\text{Pb}$ . Possible deexcitation channels at  $E^* = (25-33)$  MeV including the emission of a proton or an  $\alpha$ - particle lead to known isotopes of lawrencium with  $A \geq 254$  or nobelium with  $A \geq 252$ , which do not have intense  $\alpha$ - lines at  $E > 8700$  keV. Therefore, we tentatively assign it to an isomeric state  $^{255m}104$ , decaying via  $^{255m}104 \xrightarrow{\alpha} ^{251m}\text{No} \xrightarrow{\alpha} ^{247m}\text{Fm}$ . This suggestion is supported by the observation of the chain  $8722 \text{ keV} \rightarrow 8471 \text{ keV} \rightarrow 8126 \text{ keV}$ , since an  $\alpha$  -activity of  $E_\alpha = 8.18 \pm 0.03$  MeV and  $T_{1/2} = 9.2 \pm 2.3$  s, observed in the reaction  $^{12}\text{C} + ^{239}\text{Pu}$  at  $E_{lab} = 74$  MeV, was assigned to  $^{247m}\text{Fm}$  by Flerov et al. [24]. With respect to possible inaccuracies in the energy calibration and the deviation of our single event from the mean value an agreement is likely. The measured time difference of 3.7 s is also compatible with the half-life of  $^{247m}\text{Fm}$ . The complete data are listed in Table 1. We finally want to mention that in [5] a weak line at  $E_\alpha = 8625$  keV was attributed to  $^{255}104$ . The present experiments, however, did not give any hint of such a contribution.

The occurrence of an isomeric state having a similar half-life as the ground state, makes it of course difficult to estimate fission branches, since the assignment of the individual fission events to each of the states is hardly possible. In our recent paper [5] we obtained  $b_{sf} = 0.52 \pm 0.07$ , derived from the total numbers of observed  $\alpha$ -decays and fission events. The present value, obtained in the same way, is  $b_{sf} = 0.45 \pm 0.06$ .

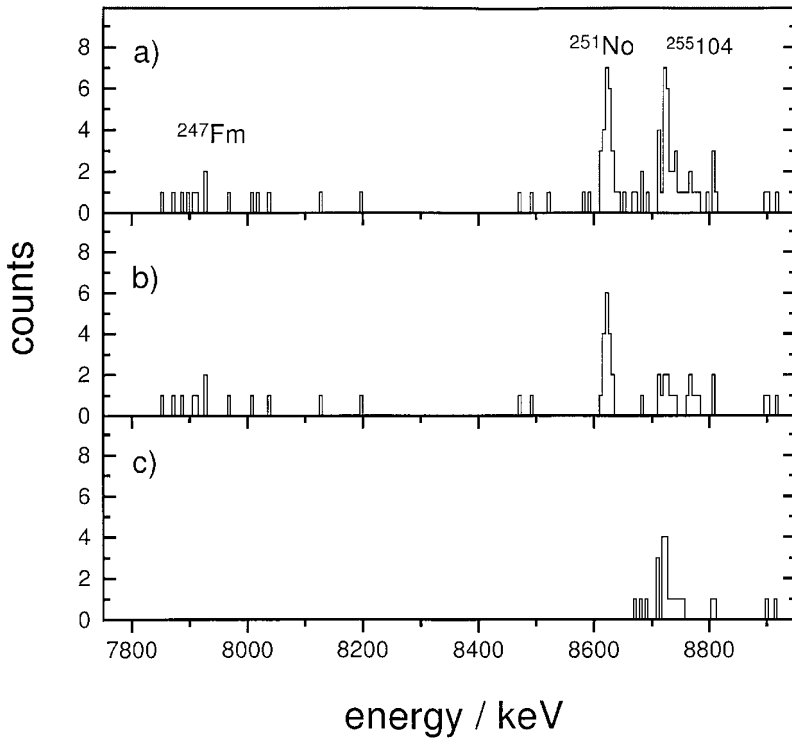


**Fig. 5.** Spectrum of  $\alpha$ -particles attributed to  $^{255}104$ ,  $^{251}\text{No}$  and  $^{247}\text{Fm}$  from  $^{50}\text{Ti} + ^{208}\text{Pb}$  at  $E = (4.90-5.10) \times A \text{ MeV}$  and  $^{50}\text{Ti} + ^{206}\text{Pb}$  at  $E = 4.81 \times A \text{ MeV}$  **a** correlated to evaporation residues **b** correlated to daughter decays  $^{251}\text{No}$  and/or  $^{247}\text{Fm}$  ( $E = 7750 - 8700 \text{ keV}$ ) **c** not correlated to daughter decays

### 3.1.5 Isotope $^{254}104$

The  $^{206}\text{Pb}$  targets were irradiated at a projectile energy of  $E_{lab} = 4.81 \times A \text{ MeV}$ , corresponding to  $E^* = 21.5 \text{ MeV}$  of the compound nucleus  $^{256}104$ . This  $E^*$  value is expected to be the optimum for the production of  $2n$ -evaporation residues according to the measured excitation function for the reaction  $^{50}\text{Ti} + ^{208}\text{Pb} \rightarrow ^{258}104$  (Sect. 3.1.1). Correspondingly, the spontaneous fission activity with  $T_{1/2} = (23 \pm 3) \mu\text{s}$  (see Fig. 6a) observed is attributed to the  $2n$  channel of the reaction, i.e. to the isotope  $^{254}104$ . Using the same target - projectile combination, Ter-Akopian et al. [9] observed a spontaneous fission activity of  $T_{1/2} \approx 0.5 \text{ ms}$ . Since this value, however, was at the lower limit obtainable with the rotating drum system used in that experiment [26], this assignment is ambiguous.

Our new half-life value agrees within a factor of 3 with that predicted by Smolanczuk et al. [27].  $\alpha$ -decay was not observed for this isotope, which corresponds, on the basis of the total number of 144 spontaneous fission events detected in our experiment to an upper limit of  $b_\alpha \leq 0.015$ . To estimate the partial half-life for  $\alpha$ -decay, we used the formula proposed by Poenaru et al. [28], including the parameter modification suggested by Rurarz [29], and an extrapolated  $Q_\alpha$ -value of  $Q_\alpha = 9.20 \text{ MeV}$ . The latter was obtained from the mass prediction of Myers and Swiatecki [30], corrected for the difference between the experimental value for  $^{256}104$  (see Sect. 3.1.3) and the predicted one according [30]. The calculation resulted in an  $\alpha$ -half-life of  $T_\alpha = 0.14 \text{ s}$ , and, together with the experimental half-life, in a semi-empirical estimate of  $b_\alpha \approx 2 \times 10^{-4}$ .

The cross-section was evaluated using the calculated SHIP efficiency of  $\epsilon = 0.4$  and the observed number of fission events corrected for the dead time of  $20 \mu\text{s}$ , due to the data acquisition system. The resulting value is  $\sigma = (2.4 \pm 0.2) \text{ nb}$ , and thus close to  $\sigma = (4.8 \pm 0.4) \text{ nb}$  for  $^{50}\text{Ti} + ^{207}\text{Pb}$  and  $\sigma_{max,2n} =$

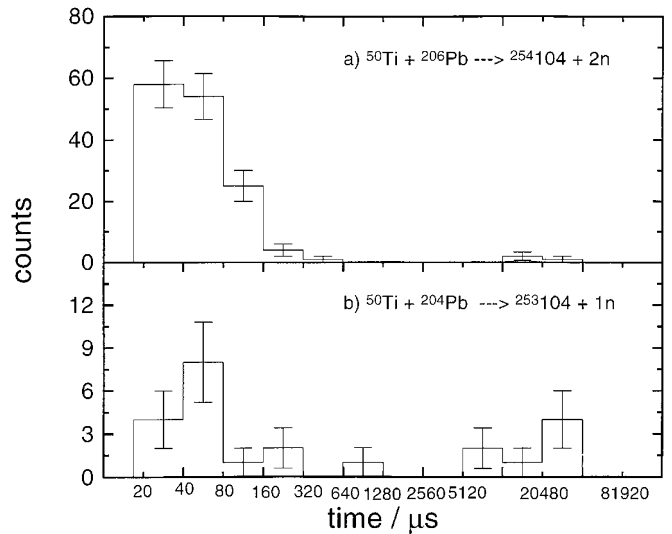


**Fig. 6.** **a** Time distribution for fission events attributed to  $^{254}104$  **b** Time distribution for fission events attributed to  $^{253}104$ . Note the constant time bins on the logarithmic scale of the abscissa

$(5.2 \pm 0.6) \text{ nb}$  for  $^{50}\text{Ti} + ^{208}\text{Pb}$  [5]. It is also comparable with the value of  $\sigma_{max,2n} = (12 \pm 1) \text{ nb}$  for  $^{50}\text{Ti} + ^{208}\text{Pb}$  from this experiment (Sect. 3.1.1). The  $1n$  cross section was measured as  $\sigma = (0.8 \pm 0.2) \text{ nb}$  and is also comparable with the value  $\sigma = (1.2 \pm 0.3) \text{ nb}$  for  $^{50}\text{Ti} + ^{208}\text{Pb}$  at the same excitation energy. We thus want to state, that neither for the  $1n$ - nor for the  $2n$ - deexcitation channel we observe a drastic decrease in the cross sections when changing the neutron number of the target by two, i.e. from  $N=126$  to  $N=124$ .

### 3.1.6 Isotope $^{253}\text{104}$

The isotope  $^{253}\text{104}$  was synthesized in an irradiation of  $^{204}\text{Pb}$  with  $^{50}\text{Ti}$ . In order to avoid significant contaminations from evaporation residues produced in reactions with heavier lead isotopes, highly enriched target material (99.73%  $^{204}\text{Pb}$ , 0.17%  $^{206}\text{Pb}$ , 0.05%  $^{207}\text{Pb}$ , and 0.06%  $^{208}\text{Pb}$ ) was used.  $E_{lab}$  was chosen to be  $4.68 \times A$  MeV, corresponding to  $E^* = 15.6$  MeV in the center of the target, i.e. close to the expected maximum of the 1n deexcitation channel according to the results for  $^{50}\text{Ti} + ^{208}\text{Pb}$  (Sect 3.1.1).

In this irradiation we observed two spontaneous fission activities: 14 events, corresponding to  $\sigma = (0.19 \pm 0.05)$  nb, with  $T_{1/2} = (48_{-10}^{+17}) \mu\text{s}$ , and 8 events, corresponding to  $\sigma = (0.11 \pm 0.04)$  nb with  $T_{1/2} = (11_{-3}^{+6})$  ms. Although the half-lives suggest an assignment to  $^{254}\text{104}$  and  $^{256}\text{104}$ , such an interpretation contradicts at least for  $^{254}\text{104}$  the systematics of cross sections measured for the 1n- and 2n- deexcitation channels in reactions  $^{50}\text{Ti} + ^{206}\text{Pb}$ ,  $^{208}\text{Pb}$ . For the low  $E^*$  value chosen,  $^{254}\text{104}$  can only be produced by  $^{206}\text{Pb}(^{50}\text{Ti}, 2n)^{254}\text{104}$  and  $^{204}\text{Pb}(^{50}\text{Ti}, \gamma)^{254}\text{104}$ . Vice versa  $^{256}\text{104}$  can be produced by  $^{206}\text{Pb}(^{50}\text{Ti}, \gamma)^{256}\text{104}$ ,  $^{207}\text{Pb}(^{50}\text{Ti}, 1n)^{256}\text{104}$ , and  $^{208}\text{Pb}(^{50}\text{Ti}, 2n)^{256}\text{104}$ , in which  $^{206,207,208}\text{Pb}$  are regarded as isotopic impurities of the target material.

In the bombardment of  $^{208}\text{Pb}$  with  $^{50}\text{Ti}$  at  $E^* \approx 15.6$  MeV the production of  $^{257}\text{104}$  was observed through the 1n - deexcitation channel with  $\sigma = (10 \pm 1)$  nb, whereas  $^{256}\text{104}$  was observed through the 2n - deexcitation channel with  $\sigma = (0.7 \pm 0.3)$  nb (Sect. 3.1.1). For the following discussion one should note, that the product of the  $\gamma$  - deexcitation channel,  $^{258}\text{104}$ , also decays by spontaneous fission with  $T_{1/2} \approx 11$  ms [16], i.e. its decay properties are similar to those of  $^{256}\text{104}$ . Thus we find that at  $E^* \approx 15.6$  MeV the 1n cross section is a factor of about fourteen higher than the sum of the 2n and a possible  $\gamma$  - cross section. Further we note at  $E^* \approx 15.6$  MeV a reduction of  $\sigma_{2n}$  by a factor of approximately fifteen compared to  $\sigma_{max,2n}$ . As for  $^{50}\text{Ti} + ^{206}\text{Pb}$   $\sigma_{max,2n}$  is about 2.4 nb, as shown above, we expect for this reaction a value of  $\sigma_{2n} \approx 150$  pb at  $E^* \approx 15.6$  MeV. Taking into account the specified contribution of  $^{206}\text{Pb}$  in the target material, a value of  $\sigma_{eff,2n} \approx 0.25$  pb from the  $^{206}\text{Pb}(^{50}\text{Ti}, 2n)^{254}\text{104}$  reaction is expected.

Therefore an assignment of the 48  $\mu\text{s}$  - activity to  $^{254}\text{104}$  can be excluded by the following arguments:

a) The measured production cross section of this activity is a factor of about 800 higher than expected for the  $^{206}\text{Pb}(^{50}\text{Ti}, 2n)^{254}\text{104}$  reaction at  $E^* \approx 15.6$  MeV with respect to the specified  $^{206}\text{Pb}$  contamination of the target.

b) At the chosen excitation energy  $\sigma_{1n}$  is expected to be a factor of fourteen higher than the sum of  $\sigma_\gamma$  and  $\sigma_{2n}$ . In the case of  $^{50}\text{Ti} + ^{206}\text{Pb}$ , 1n deexcitation leads to the known isotope  $^{255}\text{104}$  having an  $\alpha$  - branching of about 50% (Sect 3.1.4). The latter isotope was not observed, however, while in the case of  $^{50}\text{Ti} + ^{204}\text{Pb}$  an assignment to the  $\gamma$  - channel is not considered as this channel was never observed unambiguously for heavier lead isotopes.

c) A third, but somewhat weaker argument is based on the time distribution of the fission events. In Fig. 6b the distribution of the events observed in the reaction  $^{50}\text{Ti} + ^{204}\text{Pb}$  is indicated to have its maximum in the time bin  $\Delta t = (40 - 80)\mu\text{s}$ ,

while the distribution of those assigned to  $^{254}\text{104}$  decreases from the time bin  $\Delta t = (20 - 40)\mu\text{s}$  to  $\Delta t = (40 - 80)\mu\text{s}$  (Fig. 6a). Although the statistical uncertainties are large due to the small number of observed events, a half-life longer than that of  $^{254}\text{104}$  is indicated.

Contrary to the discussion on the 48  $\mu\text{s}$  - sf - activity, an assignment of the 11ms - sf - activity to  $^{256}\text{104}$  cannot be ruled out completely. The optimum reaction to produce this isotope at the chosen value of  $E^*$  is  $^{207}\text{Pb}(^{50}\text{Ti}, 1n)^{256}\text{104}$ . If we assume a cross section equal to  $\sigma_{max,1n} \approx 10$  nb as obtained for  $^{208}\text{Pb}(^{50}\text{Ti}, 1n)^{257}\text{104}$ , we end up, with respect to the specified 0.05%  $^{207}\text{Pb}$  contribution in the target material, in a value of  $\sigma \approx 5$  pb, which is indeed a factor of 22 lower than the experimental value. It should be mentioned, however, that deviations from the specified contamination of  $^{207}\text{Pb}$  may increase the production of  $^{256}\text{104}$  significantly, so a  $^{207}\text{Pb}$  contamination of  $\approx 1\%$  is already sufficient to produce the number of registered 11ms - sf - events.

It thus seems justified to attribute at least the 48  $\mu\text{s}$  - sf - activity to evaporation residues from complete fusion of  $^{50}\text{Ti}$  and  $^{204}\text{Pb}$ . According to the value of  $E^*$  chosen, products of the 1n-, 1p-, and  $1\alpha$ - deexcitation channels are the possible candidates; the  $\gamma$  - channel has already been ruled out above. 1p - deexcitation, however, leads to the known  $\alpha$  - emitter  $^{253}\text{Lr}$  [7], which does not have the measured properties. Also assignment to the  $\alpha$  - channel seems improbable, since cross sections for this channel in the order or even exceeding the values of 1n channels have never been observed in lead based reactions leading to elements  $Z > 102$ .

Therefore, we assign the 48  $\mu\text{s}$  - sf - activity to  $^{253}\text{104}$ .

### 3.1.7 Isotope $^{253}\text{No}$

$^{253}\text{No}$  was first detected by Mikheev et al. [20] in bombardments of  $^{242}\text{Pu}$  with  $^{16}\text{O}$  and  $^{239}\text{Pu}$  with  $^{18}\text{O}$ ; values of  $E_\alpha = (8.01 \pm 0.03)$  MeV and  $T_{1/2} = (105 \pm 20)$  s were reported. These results were later confirmed by Ghiorso et al. [21] who used  $^{244}\text{Cm} + ^{13}\text{C}$  and  $^{246}\text{Cm} + ^{12}\text{C}$  reactions.

Besides the main energy at  $E_\alpha = 8.01$  MeV, Mikheev et al. also discussed the existence of further  $\alpha$ - lines. A second group at  $E_\alpha = (8.06 \pm 0.03)$  MeV was present in their spectra, a definite assignment to  $^{253}\text{No}$ , however, was not made due to an 'inadequacy of the statistics' [20]. Also a possible emission of  $\alpha$ - particles with  $E_\alpha > 8.1$  MeV was not excluded, but a definite conclusion was not reached.

The  $\alpha$ -decays following the decays attributed to  $^{257}\text{104}$  in the present experiment, were mostly located in the energy interval  $E_\alpha = (7990-8090)$  keV ( $\approx 90\%$ ). A smaller fraction ( $\approx 10\%$ ) was found in the interval  $E_\alpha = (8090-8200)$  keV. According to the detector resolution the distribution in the first interval was fitted by three gaussians (Fig. 7), resulting in peaks at  $E_\alpha = 8011$  keV ( $\Delta E(\text{FWHM})=21$  keV),  $E_\alpha = 8038$  keV ( $\Delta E = 17$  keV),  $E_\alpha = 8063$  keV ( $\Delta E = 21$  keV) with roughly equal intensities. The events at  $E_\alpha = (8090-8140)$  keV can be summarized to a fourth line at  $E_\alpha = 8114$  keV, which, however, may consist of an unresolved line doublet. A few more counts ( $\approx 5\%$  of the total number of events) are observed at  $E_\alpha > 8150$  keV. Due to insufficient statistics, a division into lines is speculative. The results are listed in Table 1.

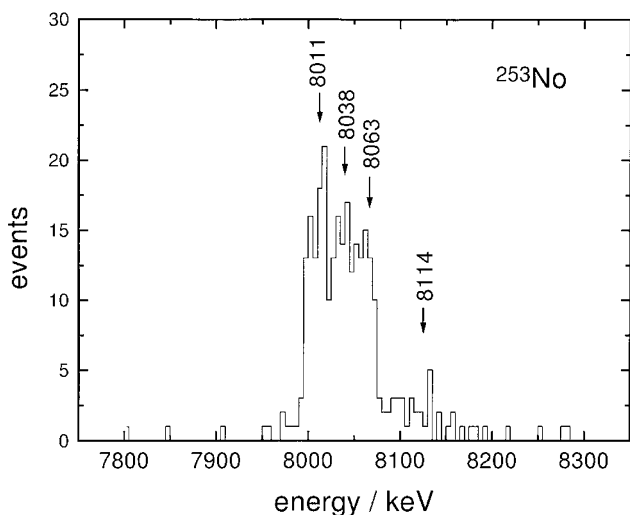


Fig. 7. Spectrum of  $\alpha$ -particles attributed to  $^{253}\text{No}$  after decay of  $^{257}104$

The correlations further exhibit some details, which could indicate a still more complicated structure of the decay patterns. On the basis of the current data a final conclusion is not possible. At this point we want to emphasize two particularities:

- there is an indication, that the events attributed to the  $E_{\alpha, \text{daughter}} = 8063$  keV - line are predominantly correlated to  $\alpha$ -decays of  $E_{\alpha, \text{mother}} > 9000$  keV.
- there is an indication for a considerable number of correlated events  $E_{\alpha, \text{mother}} = 8788$  keV  $\rightarrow$   $E_{\alpha, \text{daughter}} = 8053$  keV, slightly higher than the corresponding mean energies  $E_{\alpha} = 8779$  keV and  $E_{\alpha} = 8038$  keV.

### 3.2 Irradiations of $^{209}\text{Bi}$ with $^{51}\text{V}$ : Identification of $^{258}106$

The  $^{209}\text{Bi}$  targets were irradiated at three projectile energies,  $E_{\text{lab}} = 4.77 \times A$ ,  $4.91 \times A$ , and  $4.99 \times A$  MeV, corresponding to  $E^* = 16.1$ ,  $21.5$ , and  $24.9$  MeV of the compound nucleus  $^{260}106$ . At  $E^* = 21.5$  MeV we observed nine fission events following the implantation of a heavy nucleus within 8 ms. One event with a time distance of 1 ms and one with 25 ms, was observed at  $E^* = 24.9$  MeV and at  $E^* = 16.1$  MeV, respectively. The spontaneous fission activity was attributed to  $^{258}106$ , the 2n deexcitation channel, since its maximum production rate was found to be close to the  $E^*$  value where the measured excitation function for the similar reaction  $^{50}\text{Ti} + ^{208}\text{Pb} \rightarrow ^{258}104$  (Sect. 3.1.1) showed the maximum of the 2n deexcitation channel. It should be noted, however, that the assignment of the one fission event to  $^{258}106$  observed at the lowest excitation energy of  $E^* = 16.1$  MeV is questionable due to the time difference being three times longer than the longest time difference of the other ten events. The half-life of the spontaneous fission activity attributed to  $^{258}106$  is  $T_{1/2} = (2.9^{+1.3}_{-0.7})$  ms, neglecting the one ambiguous event at 25 ms.

$\alpha$ -decay of  $^{258}106$  was not observed, which results in an experimental upper limit  $b_{\alpha} \leq 0.2$ . Using the procedure described above for  $^{254}104$  we obtained  $Q_{\alpha} = 9.42$  MeV, which resulted in a calculated partial  $\alpha$ -half-life of  $T_{\alpha} = 165$  ms. Using the half-life calculated from the time distribution of the

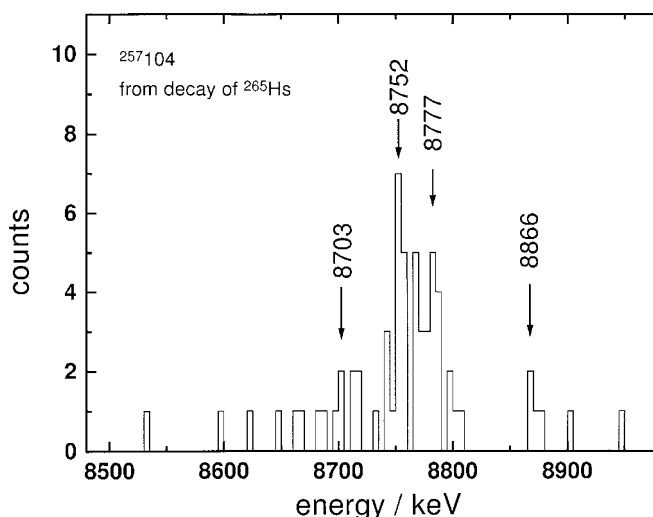


Fig. 8. Spectrum of  $\alpha$ -particles attributed to  $^{257}104$  from the decay of  $^{265}\text{Hs}$

fission events, a semi-empirical upper limit  $b_{\alpha} \leq 0.02$  is obtained. The non-observation of  $\alpha$ -decay on the basis of our number of observed fission events is thus understandable.

Our experimental half-life, which will be equated with  $T_{sf}$  in the following discussion due to the small expected  $\alpha$ -branching, is comparable to that of the neighbouring even-even nucleus  $^{260}106$  ( $T_{sf} = (7.2^{+4.8}_{-2.7})$  ms) [8], which indicates that for  $Z=106$  too the constancy of the  $T_{sf}$  is preserved on the neutron deficient side close to  $N=152$ . Our experimental value is in good agreement with the theoretical one of Smolanczuk et al. [27] who give  $T_{sf} = 1.8$  ms.

A value of  $\sigma_{\text{max}, 2n} = (38 \pm 13)$  pb was obtained at  $E^* = 21.5$  MeV. It is about an order of magnitude lower than that obtained for the neighbouring isotope  $^{259}106$  in the reaction  $^{54}\text{Cr} + ^{207}\text{Pb}$  [8], using an even-even projectile.

### 3.3 $\alpha$ -decay of $^{257}104$

Although the measured decay properties of  $^{257}104$  are in agreement with our previous results and the data of other authors, we have to point out one peculiarity that has not been explained sufficiently so far. Information on the decay properties of  $^{257}104$  was also obtained from the  $\alpha$ -decay of  $^{265}\text{Hs}$ , produced by the reaction  $^{208}\text{Pb}(^{58}\text{Fe}, 1n)^{265}\text{Hs}$  [31], where  $^{257}104$  appears as a granddaughter. A total of 65 decays of this isotope with full energy release in the stop detector was observed in the latter experiment. The energy spectrum is shown in Fig. 8. The observed  $\alpha$ -decays essentially represent three lines of  $E_{\alpha 1} = 8703$  keV,  $E_{\alpha 2} = 8752$  keV and  $E_{\alpha 3} = 8777$  keV. While  $E_{\alpha 3}$  agrees with the value of the corresponding line observed in the present experiment, differences of  $\approx 15$  keV are evident for  $E_{\alpha 1}$  and  $E_{\alpha 2}$ . More severe deviations, however, are observed for the line intensities and the half-lives. The intensities  $i(E_{\alpha 3}) : i(E_{\alpha 2}) : i(E_{\alpha 1})$  are approximately  $1 : 0.33 : 0.16$  for the  $\alpha$ -decays observed in the  $^{50}\text{Ti} + ^{208}\text{Pb}$  reaction, but  $1 : 0.84 : 0.49$  for those observed in  $^{58}\text{Fe} + ^{208}\text{Pb}$ . Half-lives are on the average approximately a factor of two longer for the products from  $^{58}\text{Fe} + ^{208}\text{Pb}$  than those of products from  $^{50}\text{Ti} + ^{208}\text{Pb}$  (Table 4). Source of the latter difference may be random correlations between 'background events' mimicking



**Table 4.** Comparison of  $\alpha$ -energies attributed to  $^{257}104$ , observed in reactions  $^{50}\text{Ti} + ^{208}\text{Pb}$  and  $^{58}\text{Fe} + ^{208}\text{Pb}$  (via  $\alpha$ -decay of  $^{265}\text{Hs}$ )

$^{50}\text{Ti} + ^{208}\text{Pb}$			$^{58}\text{Fe} + ^{208}\text{Pb}$		
$E_\alpha/\text{keV}$	$i_\alpha$	$T_{1/2}/\text{s}$	$E_\alpha/\text{keV}$	$i_\alpha$	$T_{1/2}/\text{s}$
8697	0.11	$3.5^{+1.0}_{-0.6}$	8703	0.22	$8.2^{+5.0}_{-3.2}$
8738	0.22	$4.2^{+0.8}_{-0.4}$	8752	0.40	$6.5^{+3.3}_{-2.2}$
8779	0.67	$3.5^{+0.4}_{-0.3}$	8777	0.38	$8.6^{+3.1}_{-1.8}$

evaporation residues and  $\alpha$ -particles. This background is due to scattered target-like nuclei, having initially a lower kinetic energy than evaporation residues. Since, however, we used a degrader foil in front of the detectors to absorb the scattered low energy projectiles that pass SHIP, the evaporation residues appear in the bulk of the energy distribution of those 'background events' due to their higher energy loss. To check the influence of such random correlations, we estimated their 'half-life'  $T_{rand}$  from the time distances of these 'background events' to  $\alpha$ -decays of  $^{253}\text{No}$ . A value of  $T_{rand} \approx 9$  s was obtained. Therefore we have to take into account that part of the observed evaporation residue -  $\alpha(^{257}104)$  correlations are random, i.e. we correlated the  $\alpha$ -decay to 'background' events implanted after the evaporation residue, and thus obtained a shorter half-life. In the reaction  $^{58}\text{Fe} + ^{208}\text{Pb}$  the situation was different: the half-lives were determined from the time distances between the  $\alpha$ -decays of  $^{261}106$  and  $^{257}104$ . Due to a negligible background of  $\alpha$ -decays correlation times up to several hundreds of seconds were possible.

It is further evident that for  $^{58}\text{Fe} + ^{208}\text{Pb}$  practically all  $^{257}104$  events are found in the region  $E_\alpha = (8700-8800)$  keV. Only one  $\alpha$ -decay of  $^{261}106$  was found to be followed by an event of  $E_\alpha > 8900$  keV, while about 60% of the decays of  $^{257}104$ , produced by the reaction  $^{208}\text{Pb}(^{50}\text{Ti},1n)^{257}104$  are found in this energy region. This experimental result suggests the existence of an isomeric state in  $^{257}104$ , not populated by  $\alpha$ -decay of  $^{261}106$ , decaying by  $\alpha$ -emission with energies of essentially  $E_\alpha = 9021$  keV and  $E_\alpha = 8968$  keV. One also could speculate about a third  $\alpha$ -line from the isomeric state, being the origin of the different line intensities discussed above. Such an assumption, however, is presently not well founded.

The assumption of an isomeric state in  $^{257}104$  is further supported by a comparison of the  $\alpha$ -decay patterns of the N=153 nuclei  $^{257}104$ ,  $^{255}\text{No}$  and  $^{253}\text{Fm}$  (Fig. 9). Disregarding the lines at  $E_\alpha = 9021$  keV and  $E_\alpha = 8968$  keV and taking the line at  $E_\alpha = 8903$  keV as the ground state transition we obtain for  $^{257}104$  a pattern as shown in Fig. 9. All three patterns start with two weak lines having energy differences  $\Delta E \approx (40-60)$  keV, containing less than 10% of the total intensity and having hindrance factors  $\gg 100$ . The bulk of the intensity ( $i_{rel} > 0.60$ ) is concentrated in a triplet (at  $^{253}\text{Fm}$  a weak fourth line is indicated), starting at  $|\Delta E| > 120$  keV from the line representing the ground state decay. Hindrance factors of corresponding lines are equal within a factor of two. Highest intensities ( $i \approx (0.4-0.5)$ ) are observed for the first lines of the triplets. These schemes reflect a similar nuclear structure for these odd neutron nuclei differing just by two protons. The two high energy lines of  $^{257}104$  do not fit in these schemes, so an origin different from ground state decay is likely.

A more thorough discussion of this subject can be explored by means of level schemes of N=153 and N=151 isotones ei-

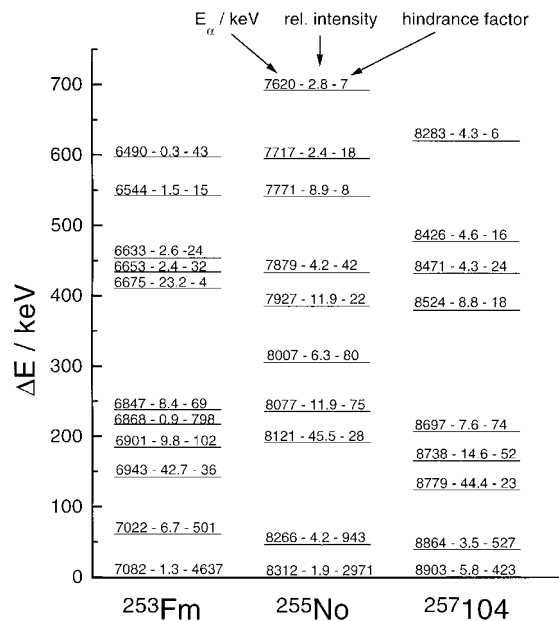


**Fig. 9.**  $\alpha$ -decay patterns for  $^{257}104$ ,  $^{255}\text{No}$ , and  $^{253}\text{Fm}$ . The ordinate represents the energy difference with respect to the decay energy attributed to the groundstate transition. For each level, the first number represents the  $\alpha$ -decay energy, the second one the relative intensity, and the third one the hindrance factor.  $\alpha$ -decay energies and relative intensities for  $^{255}\text{No}$  and  $^{253}\text{Fm}$  were taken from the literature [32]. Theoretical  $\alpha$ -half-lives were calculated according to [28]

ther determined experimentally [32] or calculated [33]. Corresponding levels are listed in Table 5. The following tendencies are evident: the groundstate of N=153 isotones is given as  $1/2^+[620]$ , the first excited Nilsson - levels as  $7/2^+[613]$ ,  $3/2^+[622]$ ,  $11/2^- [725]$  and  $9/2^- [734]$ . The calculations further indicate a slight increase of the  $7/2^+[613]$  level with increasing atomic number, while the  $11/2^- [725]$  level decreases. At Z=104 the  $11/2^- [725]$  level lies below the  $7/2^+[613]$  according to the calculations.  $\gamma$ -decay from the  $11/2^- [725]$  can be assumed to be strongly spin hindered, so an isomeric state decaying by  $\alpha$  emission would not be unexpected. It should be noted, however, that for  $^{251}\text{Cf}$  the experimental results settle the  $7/2^+[613]$  level below the  $3/2^+[622]$ , just the reverse of the order resulting from the calculations.

The groundstate of N=151 isotones is given as  $9/2^- [734]$  [32]. The first excited Nilsson - levels are given as  $5/2^+[622]$ ,  $7/2^+[624]$  ( $7/2^+[613]$  for  $^{251}\text{Fm}$ ) and  $1/2^+[620]$  [32]. The levels  $5/2^+[622]$  and  $7/2^+[624]$  are exchanged in the calculations compared to the experimental assignment. The  $1/2^+[620]$  - level (which is the groundstate of the N=153 isotones) is positioned  $\approx (400-450)$  keV above the groundstate according to the experimental results, while calculations indicate values of  $\approx (600-700)$  keV. As a consequence of this behavior  $\alpha$ -decays from N=153 isotones to the Nilsson level in the daughter corresponding to that of the groundstate of the mother nuclei ('favored transitions') are hindered by unfavorable Q-values. Thus they are not expected to have the highest transition rates.

The highest intensities are observed for decays into the  $5/2^+[622]$  daughter level. Therefore, as a rule, we observe the following decay pattern: two weaker lines, representing the decays into the lowest levels  $9/2^- [734]$  and  $11/2^- [734]$ , are

**Table 5.** Comparison of experimental [32] and calculated [33] level order for a) N=153 isotones and b) N=151 isotones

$^{251}\text{Cf}$				$^{253}\text{Fm}$				$^{255}\text{No}$				$^{257}\text{104}$			
exp		calc		calc		calc		exp		calc		exp		calc	
$I^\pi[\text{Nn}_zA]$	E/keV	$I^\pi[\text{Nn}_zA]$	E/keV	$I^\pi[\text{Nn}_zA]$	E/keV	$I^\pi[\text{Nn}_zA]$	E/keV	$I^\pi[\text{Nn}_zA]$	E/keV	$I^\pi[\text{Nn}_zA]$	E/keV	$I^\pi[\text{Nn}_zA]$	E/keV	$I^\pi[\text{Nn}_zA]$	E/keV
$1/2^+[620]$	gs	$1/2^+[620]$	gs	$1/2^+[620]$	gs	$1/2^+[620]$	gs	$1/2^+[620]$	gs	$1/2^+[620]$	gs	$1/2^+[620]$	gs	$1/2^+[620]$	gs
$7/2^+[613]$	106	$7/2^+[613]$	178	$3/2^+[622]$	111	$3/2^+[622]$	98	$11/2^- [725]$	118	$11/2^- [725]$	118	$3/2^+[622]$	85	$11/2^- [725]$	207
$3/2^+[622]$	178	$3/2^+[622]$	123	$7/2^+[613]$	239	$7/2^+[613]$	277	$7/2^+[613]$	286	$7/2^+[613]$	286	$7/2^+[613]$	279	$9/2^- [734]$	459
$11/2^- [725]$	370	$11/2^- [725]$	372	$11/2^- [725]$	333	$9/2^- [734]$	384	$9/2^- [734]$	442						
$9/2^- [734]$	434	$9/2^- [734]$	423												

$^{247}\text{Cm}$				$^{249}\text{Cf}$				$^{251}\text{Fm}$				$^{253}\text{No}$			
exp		calc		exp		calc		exp		calc		exp		calc	
$I^\pi[\text{Nn}_zA]$	E/keV	$I^\pi[\text{Nn}_zA]$	E/keV	$I^\pi[\text{Nn}_zA]$	E/keV	$I^\pi[\text{Nn}_zA]$	E/keV	$I^\pi[\text{Nn}_zA]$	E/keV	$I^\pi[\text{Nn}_zA]$	E/keV	$I^\pi[\text{Nn}_zA]$	E/keV	$I^\pi[\text{Nn}_zA]$	E/keV
$9/2^- [734]$	gs	$9/2^- [734]$	gs	$9/2^- [734]$	gs	$9/2^- [734]$	gs	$9/2^- [734]$	gs	$9/2^- [734]$	gs	$9/2^- [734]$	gs	$9/2^- [734]$	gs
$5/2^+[622]$	227	$7/2^+[624]$	216	$5/2^+[622]$	145	$7/2^+[624]$	221	$5/2^+[622]$	190	$7/2^+[624]$	211	$5/2^+[622]$	124	$7/2^+[624]$	237
$7/2^+[624]$	285	$5/2^+[622]$	527	$7/2^+[624]$	380	$5/2^+[622]$	488	$7/2^+[613]$	400	$5/2^+[622]$	444	$7/2^+[624]$	379	$5/2^+[622]$	414
$1/2^+[620]$	404	$1/2^+[620]$	589	$1/2^+[620]$	417	$1/2^+[620]$	623	$1/2^+[620]$	550	$1/2^+[620]$	649	$1/2^+[620]$	620	$1/2^+[620]$	671

followed by intense decays into the  $5/2^+[622]$  level, which again is followed by two weaker lines from the decays into the  $7/2^+[622]$  and  $9/2^+[622]$  levels, the next members of the rotational band.

According to this rule, we assign the lines at  $E_\alpha = 8903$  keV and  $E_\alpha = 8864$  keV to the decays into the groundstate rotational band, the lines at  $E_\alpha = 8779$  keV,  $E_\alpha = 8738$  keV and  $E_\alpha = 8697$  keV to the band built up on the  $5/2^+[622]$  level. The assignment of the residual decays is less certain. The following levels are  $7/2^+[624]$  ( $7/2^+[613]$ ) for  $^{251}\text{Fm}$  and  $1/2^+[620]$ . Although uncertainties are large due to the low number of observed events we will make a tentative assignment on the basis of the hindrance factors and level schemes for the N=151 isotones: the favored transition is assigned to the  $\alpha$  - line having the lowest hindrance factor, i.e.  $E_\alpha = 8283$  keV (HF = 5.9), while the line at  $E_\alpha = 8524$  keV is attributed to the decay into the  $7/2^+[624]$  level.

The isomeric state  $^{257m}\text{104}$  is assigned to the  $11/2^- [725]$  Nilsson orbital.  $\gamma$ -decay to the ground state is strongly suppressed due to the high spin difference of  $\Delta I = 5$ . An estimation on the daughter level of the isomeric decay can be given on the basis of the hindrance factors. An experimental partial half-life of  $T_{\alpha,exp} \approx 8$  s is obtained for the  $E_\alpha = 9021$  keV - line, while calculations indicate a value of  $T_{\alpha,calc} \approx 0.18$  s, resulting in a hindrance of  $\approx 40$ . Such a value is meaningful for a  $11/2^- [725] \rightarrow 9/2^- [734]$  transition, but is definitely too low for transitions into one of the low lying excited states, since these transitions are accompanied by both, a change of the principal quantum number and a change of the parity. The excitation energy of the  $11/2^- [725]$  - level can be estimated from the differences of  $Q_\alpha$  - values for decays from the ground-state and the isomeric state to the  $9/2^- [734]$  - ground state in  $^{253}\text{No}$ . A value of  $E_{ex} = (118 \pm 4)$  keV is obtained. The proposed decay scheme is sketched in Fig. 10.

#### 4 Summary and conclusion

In the course of our experiments three new fission activities have been identified in the reactions  $^{51}\text{V} + ^{209}\text{Bi}$  and  $^{50}\text{Ti} + ^{204,206}\text{Pb}$ .

In the bombardment of  $^{209}\text{Bi}$  with  $^{51}\text{V}$  the so far lightest isotope of element 106,  $^{258}\text{106}$  was identified. Its measured

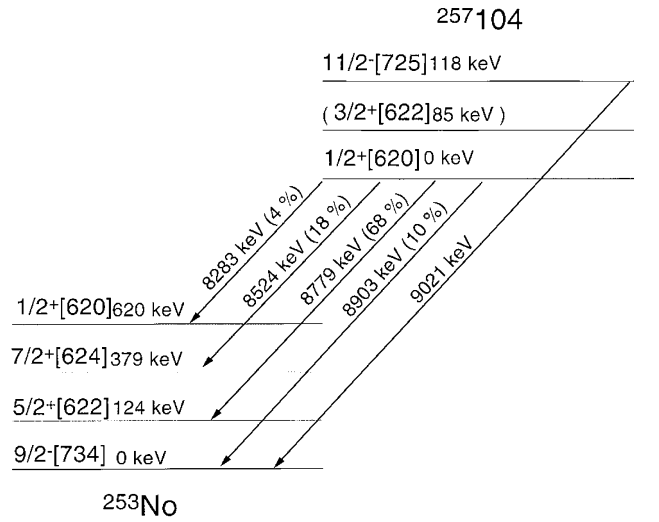


**Fig. 10.** Sketch of the decay scheme proposed for  $^{257}\text{104}$ . Only the decays into the band heads are indicated for better presentation. Level energies are based on the differences of the experimental  $\alpha$ -energies. The intensities for a given Nilsson-orbital represent the sum of all decay branches observed for that state

half-life of  $T_{1/2} = (2.9_{-0.7}^{+1.3})$  ms, which roughly is only a factor of two lower than that of the neighbouring even-even isotope  $^{260}\text{106}$ , demonstrates that the stabilisation of nuclei against fission due to the N=152 subshell is still active for Z=106.

Two more new spontaneous fission activities of  $T_{1/2} = (48_{-10}^{+17}) \mu\text{s}$  and  $T_{1/2} = (23 \pm 3) \mu\text{s}$ , observed in irradiations of  $^{204,206}\text{Pb}$  with  $^{50}\text{Ti}$ , were attributed to  $^{253}\text{104}$  and  $^{254}\text{104}$ , respectively. These results prove a drastic decrease of fission half-lives for element 104 isotopes with  $N < 152$ , as is also predicted by calculations [27]. Responsible for this behavior are both: decreasing fission barrier heights due to a rapid decrease of nuclear shell effects [27, 34], and a reduction of the width of the single humped fission barrier [35].

Improved  $\alpha$ -decay data for  $^{255}\text{104}$  were obtained. The results strongly suggest the existence of isomeric states in  $^{255}\text{104}$  and  $^{251}\text{No}$  decaying by  $\alpha$  - emission.

The  $\alpha$ -decay energies and intensities observed for  $^{257}\text{104}$  were compared to literature values for lighter N=153 isotones.

An isomeric state  $^{257m}104$  decaying by  $\alpha$  - emission could be identified. The results were also used to draw up a first rough level scheme for  $^{257}104$  and  $^{253}\text{No}$ .

## References

- Ghiorso, A.: Proceedings of the Robert A. Welch Foundation Conference on Chemical Research, XIII. The Transuranium Elements - The Mendeleev Centennial, November 17-19, 1969, Houston, Texas, **143** (1970)
- Türler, A., Gäggeler, H.W., Jost, D.T., Armbruster, P., Bröchle, W., Folger, H., Heßberger, F.P., Hofmann, S., Münzenberg, G., Ninov, V., Schädel, M., Sümmerer, K., Kratz, J.V., Scherer, U.: Z. Phys. A - Atomic Nuclei **331**, 363 (1988)
- Oganessian, Yu.Ts., Iljinov, A.S., Demin, A.G., Tretyakova, S.P.: Nucl. Phys. **A239**, 353 (1975)
- Viola Jr., V.E., Mignerey, A.C., Breuer, H. Wolf, K.L., Glagola, B.G., Wilcke, W.W., Schröder, U., Huizenga, J.R., Hilscher, D., Birkelund, J.R.: Phys. Rev. **C22**, 122 (1980)
- Heßberger, F.P., Münzenberg, G., Hofmann, S., Reisdorf, W., Schmidt, K.-H., Schött, H.J., Armbruster, P., Hingmann, R., Thuma, B., Vermeulen, D.: Z. Phys. A - Atoms and Nuclei **321**, 317 (1985)
- Heßberger, F.P., Münzenberg, G., Hofmann, S., Armbruster, P., Agarwal, Y.K., Reisdorf, W., Poppensieker, K., Schmidt, K.-H., Schneider, J.R.H., Schneider, W.F.W., Schött, H.J., Sahn, C.-C., Vermeulen, D., Thuma, B.: Journal of Less-Common Metals, **122**, 445 (1986)
- Heßberger, F.P., Münzenberg, G., Hofmann, S., Agarwal, Y.K., Poppensieker, K., Reisdorf, W., Schmidt, K.-H., Schneider, J.R.H., Schneider, W.F.W., Schött, H.J., Armbruster, P., Leino, M.E., Hingmann, R.: Z. Phys. A - Atoms and Nuclei **322**, 227 (1985)
- Münzenberg, G., Hofmann, S., Folger, H., Heßberger, F.P., Keller, J., Poppensieker, K., Quint, B., Reisdorf, W., Schmidt, K.-H., Schött, H.J., Armbruster, P., Thuma, B., Sahn, C.-C., Vermeulen, D.: Z. Phys. A - Atoms and Nuclei **322**, 557 (1985)
- Ter-Akopian, G.M., Iljinov, A.S., Oganessian, Yu.Ts., Orlova, A., Popeko, G.S., Tretyakova, S.P., Chepigina, V.I., Shilov, B.V., Flerov, G.N.: Nucl. Phys. **A255**, 509 (1975)
- Folger, H., Hartmann, W., Heßberger, F.P., Hofmann, S., Klemm, J., Münzenberg, G., Ninov, V., Thalheimer, W., Armbruster, P.: Nucl. Instrum. Methods in Phys. Res. **A362**, 65 (1995)
- Münzenberg, G., Faust, W., Hofmann, S., Armbruster, P., Güttner, K., Ewald, H.: Nucl. Instrum. Methods **161**, 65 (1979)
- Saro, S., Janik, R., Hofmann, S., Folger, H., Heßberger, F.P., Ninov, V., Schött, H.J., Andreyev, A.N., Popeko, A.G., Kabachenko, A.P., Yeremin, A.V.: Nucl. Instr. Meth. in Phys. Res. **A381**, 520 (1996)
- Hofmann, S., Ninov, V., Heßberger, F.P., Folger, H., Münzenberg, G., Schött, H.J., Armbruster, P., Popeko, A.G., Yeremin, A.V., Andreyev, A.N., Saro, S., Janik, R., Leino, M.E.: Z. Phys. **A350**, 277 (1995)
- Audi, G., Wapstra, A.H.: Nucl. Phys. **A565**, 1 (1993)
- Hubert, F., Bimbot, R., Gauvin, H.: At. Data and Nucl. Data Tables **46**, 1, 1 (1990)
- Ghiorso, A., Nurmia, M., Harris, J., Eskola, K., Eskola, P.: Phys. Rev. Lett. **22**, 1317 (1969)
- Bemis Jr., C.E., Silva, R.J., Hensley, D.C., Keller Jr., O.L., Tarrant, J.R., Hunt, L.D., Dittner, P.F., Hahn, R.L., Goodman, C.D.: Phys. Rev. Lett. **31**, 647 (1973)
- Eskola, K., Eskola, P., Nurmia, M., Ghiorso, A.: Phys. Rev. **C4**, 632 (1971)
- Bemis Jr., C.E., Hensley, D.C., Dittner, P.F., Hahn, R.L., Silva, R.J., Tarrant, J.R., Hunt, L.D.: ORNL-5137, **73** (1976)
- Mikheev, V.L., Ilyushchenko, V.I., Miller, M.B., Polikanov, S.M., Flerov, G.N., Kharitonov, Yu.P.: Atomnaya Energiya **22**, 90 (1967)
- Ghiorso, A., Sikkeland, T., Nurmia, M.: Phys. Rev. Lett. **18**, 401 (1967)
- Somerville, L.P., Nurmia, M.J., Nitschke, J.M., Ghiorso, A., Hulet, E.K., Lougheed, R.W.: Phys. Rev. **C31**, 1801 (1985)
- Heßberger, F.P.: GSI-Report GSI-85-11 (1985)
- Flerov, G.N., Polikanov, S.M., Mikheev, V.L., Ilyushchenko, V.I., Miller, M.B., Shchegolev, V.A.: Atomnaya Energiya **22**, 342 (1967)
- Heßberger, F.P., Hofmann, S., Münzenberg, G., Hofmann, S., Schmidt, K.-H., Armbruster, P., Hingmann, R.: Nucl. Instr. Meth. in Phys. Res. **A274**, 522 (1989)
- Ter-Akopian, G.M.: private communication 1994
- Smolanczuk, R., Skalski, J., Sobiczewski, A.: Phys. Rev. **C52**, 1871 (1995)
- Poenaru, D.N., Ivancu, M., Mazila, M.: J. Physique Lett. **41**, 589 (1980)
- Ruraz, E.: Acta Physica Polonica **B14**, 12, 917 (1984)
- Myers, W.D., Swiatecki, W.J.: Nucl. Phys. **A601**, 141 (1996)
- Ninov, V. et al.: to be published
- Firestone, R.B., Shirley, V.S. (editors): Table of Isotopes 8th edition, John Wiley & sons, inc. New York, Chichester, Brisbane, Toronto, Singapore (1996)
- Cwiok, S., Hofmann, S., Nazarewicz, W.: Nucl. Phys. **A573**, 356 (1994)
- Möller, P., Nix, R.J., Myers, W.D., Swiatecki, W.J.: At. Data and Nucl. Data Tables **59**, 185 (1995)
- Möller, P.: Int. Meeting on Reaction of Heavy Ions and Synthesis of New Elements, Dubna, December 13-16, 1977 (unpublished)
- Lane, M.R., Gregorich, K.E., Lee, D.M., Mohar, M.F., Hsu, M., Kacher, C.D., Kadkhodayan, B., Neu, M.P., Stoyer, N.J., Sylwester, E.R., Yang, J.C., Hoffman, D.C.: Phys. Rev. **C53**, 2893 (1996)
- Schädel, M., Bröchle, W., Schausten, B., Schimpf, E., Jäger, E., Wirth, G., Günther, R., Kratz, J.V., Paulus, W., Seibert, A., Thörle, P., Trautmann, N., Zauner, S., Schumann, D., Andrassy, M., Misiak, R., Gregorich, K.E., Hoffman, D.C., Lee, D.M., Sylwester, E.R., Nagame, Y., Oura, Y.: Radiochimica Acta **77**, 149 (1997)